

RESEARCH ARTICLE | JANUARY 30 2012

Spectroscopic reflectometry of mirror surfaces during plasma exposure

M. Wisse; B. Eren; L. Marot; R. Steiner; E. Meyer



Rev Sci Instrum 83, 013509 (2012)

<https://doi.org/10.1063/1.3678640>



CrossMark

Spectroscopic reflectometry of mirror surfaces during plasma exposure

M. Wisse,^{a)} B. Eren, L. Marot, R. Steiner, and E. Meyer

Department of Physics, University of Basel, Klingelbergstrasse 82, CH-4056, Basel, Switzerland

(Received 22 September 2011; accepted 3 January 2012; published online 30 January 2012)

An *in situ* spectroscopic reflectometry system has been built to investigate the evolution of the specular reflectivity spectrum of ITER first mirror samples during plasma exposure. Results are presented for three different types of molybdenum mirror samples that were exposed to deuterium plasma, including single crystalline, nanocrystalline, and polycrystalline molybdenum. The results show good agreement with *ex situ* measurements of the reflectivity spectrum before and after exposure and extend the results obtained in previous experiments. © 2012 American Institute of Physics. [doi:10.1063/1.3678640]

I. INTRODUCTION

In ITER, the most crucial element of each optical system is the first mirror in the optical path, which serves to guide light into the mirror labyrinth leading to the diagnostic outside the neutron shielding. Being close to the plasma, the first mirrors may be subject to erosion and/or deposition, depending on their exact location in the machine. Both erosion and deposition will affect the reflectivity of the mirror surface, compromising the measurements. These conditions pose a challenge to finding a suitable material, which is still an ongoing effort.¹ Presently, molybdenum is considered to be the strongest candidate on account of its low sputtering yield, providing some resilience to erosion by charge-exchange neutrals, and adequate reflectivity.² One of the key questions to address concerns the evolution of the reflectivity spectrum under conditions such as might be expected in ITER. One aspect that needs considering is the behaviour of the reflectivity under pure deuterium plasma exposure, as this is relevant both for mirrors in erosion dominated zones as well as for mirrors in deposition dominated zones subjected to plasma cleaning, which is currently being considered as a possible means to clean mirrors *in situ*. Our previous work³ showed that after an initial deterioration, molybdenum exhibits a stable reflectivity spectrum under continued deuterium plasma exposure; an effect we attributed to the presence of deuterium and deuterium induced defects in the subsurface. These results were obtained from measurements of the reflectivity before and after exposure, though the range of different exposure times did provide some temporal information. However, in addition to that, the reflectivity measurements were made *ex situ*. This means that changes due to effects that occurred after exposure, such as oxidation, will affect the result. Also effects that may only be persistent while in vacuum, such as hydride formation, cannot be accounted for. In order to address these points, a new *in situ* spectroscopic reflectometry system has been developed that monitors the relative reflectivity between 400 and 800 nm during exposure.

^{a)} Author to whom correspondence should be addressed. Electronic mail: marco.wisse@unibas.ch.

II. PLASMA EXPOSURE FACILITY

The plasma exposure facility at the University of Basel offers a complete toolkit for the manufacturing and investigation of metallic mirrors, including experimental simulation of erosion and deposition conditions that are likely to occur in ITER. This is supplemented by an extended set of diagnostics for chemical surface analysis and optical surface characterisation as well as plasma diagnostic tools, including *in situ* x ray and UV photoelectron spectroscopy (PES) and *ex situ* spectroscopic ellipsometry and spectrophotometry. The setup, shown in Fig. 1, is constructed around a high vacuum chamber equipped with an RF plasma source and magnetrons, allowing the injection of various types of gases and the admixture of impurities through magnetron sputtering. Conventional pumping systems are used to obtain a background pressure of typically 1.5×10^{-4} Pa. Plasma is created in a Pyrex tube of 12 cm diameter and 40 cm length through a matching network by a 13.56 MHz RF generator at a typical power of 90 W. This RF power is coupled to the tube by an outer electrode acting as a surfatron. At the heart of the chamber is a sample carousel with heatable and biasable probe holders, which typically take samples of 25 mm diameter. The small diameter compared to the diameter of the plasma source ensures homogeneity of the plasma across the sample surface. A PES spectrometer is attached to the vacuum chamber, allowing samples to be transferred directly for chemical surface analysis after exposure. A mass spectrometer, a Langmuir probe and an optical spectrometer are used for plasma analysis.

III. IN SITU SPECTROSCOPIC REFLECTOMETRY

The question of the temporal evolution of the reflectivity spectrum of metal mirrors during plasma exposure, either under ITER relevant erosion or deposition conditions or for the purpose of plasma cleaning, motivated the design of an *in situ* spectroscopic reflectometry system.

The reflectometer, shown in Fig. 2, is built around two identical AVANTES USB spectrometers (Avaspec 2048-USB2-UA). This is a commercial fibre-coupled reflection grating spectrometer with a usable wavelength range from 200 to 1100 nm. The grating has 300 lines/mm. A 2048 pixel

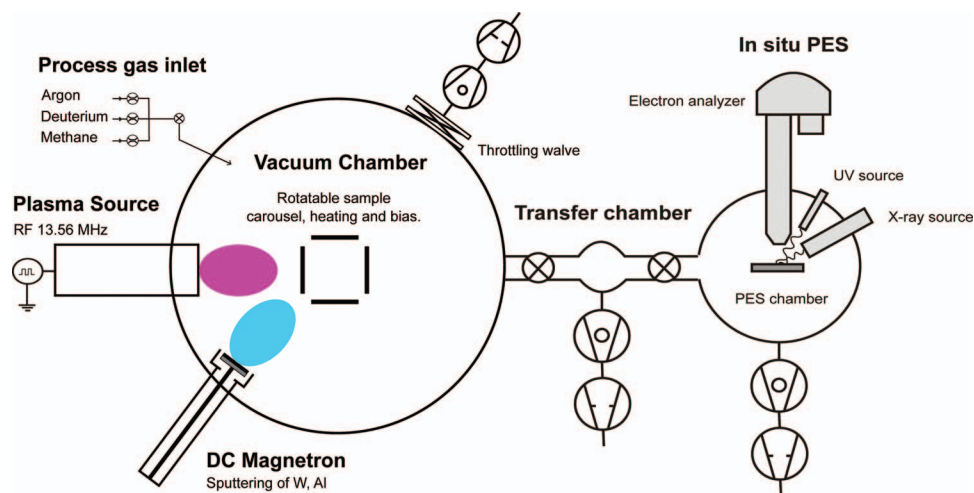


FIG. 1. (Color online) Plasma exposure facility, consisting of a high vacuum chamber with RF plasma source, magnetrons and in situ PES spectrometer.

linear ccd detector captures light at $f/7.5$, with a minimum exposure time of 1.1 ms. A 16 bit analog-to-digital converter (ADC) is used, with an offset between 1000 and 2000 counts, depending on the spectrometer. At room temperature, the dark current is typically 2 counts/ms. A $50\ \mu\text{m}$ slit is installed behind the fibre entrance. A 150 W fibre coupled tungsten halogen light source (Schott KL1500 Compact) is used to couple light into a 3 mm fibre bundle, the exit of which is in the focal plane of a 2" collimating lens ($f = 150\ \text{mm}$). A wedged beam sampler reflects a part of the collimated beam, typically 4%, which travels back through the collimating lens towards a 1" 50° engineered diffuser (Thorlabs), behind which a $400\ \mu\text{m}$ fibre collects the light and feeds it to one of the spectrometers. This reference signal allows the reflected signal to be corrected for changes in the intensity of the light source that may occur during the plasma exposures, which typically take several hours. The main part of the beam is focused by a second lens onto a 10 mm spot on the sample surface.

After being reflected by the sample, the beam exits the vacuum chamber and is collected by a 2" integrating sphere coupled to another $400\ \mu\text{m}$ fibre, which is connected to the second spectrometer. The integrating sphere makes the system insensitive to small changes in the alignment that typically occur when heating the sample to 150°C , which is the temperature at which the plasma exposures typically take place. The high power light source ensures that the plasma light has a negligible influence on the measurement and a shutter was deemed unnecessary, though one may be implemented in the future to allow for real time dark current correction.

In order to minimise the effect of instabilities in the light source or mechanical perturbation of the fibre affecting the angular distribution emanating from the fibre exit, a 1" 20° engineered diffuser is placed at the fibre exit. This results in a small (10%) loss of light, but enhances the stability of the angular distribution. The current light source allows for measurements to be made in the visible between 400 and 800 nm. A LabVIEW program is used for data acquisition.

A typical measurement proceeds as follows. An integration time is chosen for each spectrometer, such that the signal reaches about 80%–90% of the maximum number of counts allowed by the 16 bit limit. This results in a typical integration time of 120 ms for the spectrometer sampling of the reflected beam, and 40 ms for the one sampling of the reference beam. A number of averages are then chosen for each, such that the total integration time per recorded spectrum is equal for both spectrometers. The ADC offset, which is known for each spectrometer, is subtracted automatically prior to storing the spectra. The dark current at 120 ms integration time is 200–300 counts at room temperature, vs. 55 000 counts of typical signal. As both spectrometers offer the possibility of automatic dark current correction, this feature is enabled by default during our measurements, though the dark current may be regarded as negligible for our purposes. The system has not been absolutely calibrated and is thus used to measure the evolution of the reflectivity spectrum relative to the first time slice. That is to say that we are interested in the quantity $\tilde{R}(\lambda, t) = I_s(\lambda, t)/I_s(\lambda, 0)$, where $I_s(\lambda, t)$ is the number of counts at time t and wavelength λ measured by

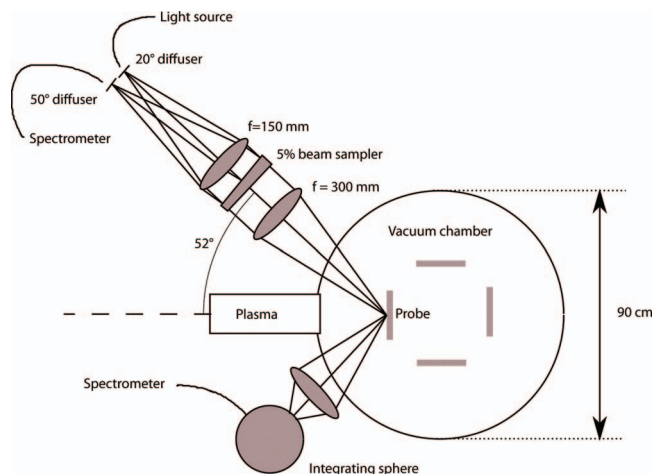


FIG. 2. (Color online) Layout of the reflectometer. Light is coupled from a 150 W light source into a 3 mm light guide and focused on the sample. A few percent of the ingoing beam is sampled by a spectrometer and used to correct the reflected signal for variations in the intensity of the ingoing beam. The reflected light is collected using a 2" integrating sphere coupled to a second spectrometer.

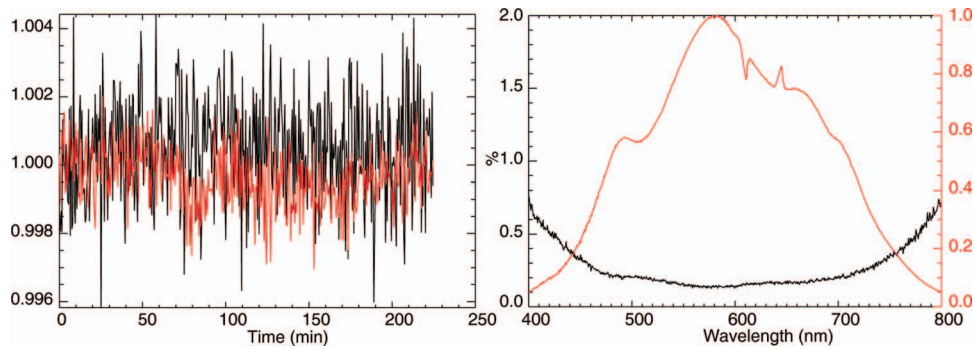


FIG. 3. (Color online) (a) Time trace of the intensity at 575 nm of the reflected beam (black) and the reference beam (red), relative to the first time slice, measured without plasma exposure. (b) Standard deviation of the derived value of the reflectivity, relative to the first time slice, divided by the mean value (black). A sample spectrum with arbitrary units is shown in red.

the spectrometer sampling the reflected beam. $I_s(\lambda, 0)$ is the first time slice, which is actually an average of a number of time slices taken prior to starting the plasma, in order to reduce the statistical uncertainty induced by photon noise. To correct for intensity fluctuations of the light source that occur during the plasma exposures, which typically take several hours, the reflected spectrum at each time slice is divided by the reference spectrum, normalised to its first time slice: $\tilde{R}(\lambda, t) \rightarrow \tilde{R}(\lambda, t)I_r(\lambda, t)/I_r(\lambda, 0)$, where $I_r(\lambda, t)$ is the number of counts measured by the reference spectrometer and $I_r(\lambda, 0)$ is the average of a number of time slices taken before starting the exposure. As there is not an exact one-to-one correspondence between the pixels to wavelength conversion and between both spectrometers, the reference spectrum is interpolated to match the wavelength axis of the other spectrometer prior to performing the correction. However, wavelength calibration of both spectrometers with a mercury lamp has demonstrated excellent correspondence between the wavelength axes.

A possible source of error could have been the plasma light. However, due to the short integration time (~ 120 ms) allowed by the high power light source and the presence of the integrating sphere, the plasma light is invisible even at the D-alpha wavelength where it is strongest.

Neglecting the contribution of the dark current to the error on the derived relative reflectivity, the main source of statistical error is the photon noise on each spectrum, which is proportional to the square root of the number of counts. This is easily quantified by performing a measurement on a sample without exposing it to the plasma, for an extended period of time and measuring the rms fluctuation on the derived value of \tilde{R} . The result of such a measurement is shown in Fig. 3, which demonstrates that the rms variation is below 0.5% for most of the region between 400 and 800 nm, where the photon count is sufficiently high. It should be emphasized that this measurement relies on the change of the specular reflectivity being identical for s- and p-polarized light, as a certain amount of polarization of the incident beam is to be expected due to the fact that it travels through two windows that are not perpendicular to the beam and therefore induce a certain amount of polarization. Therefore, in order for the measured relative change in intensity to represent the relative change in specular reflectivity, the relative change of the s and p components must be identical. However, this assumption is of minor con-

cern for the purpose of this measurement, as even its violation would be a lower order effect than the one this measurement aims to determine, that is the behaviour of the specular reflectivity without distinguishing between the polarization components. The good agreement between *ex situ* measurements performed with a spectrophotometer before and after exposure, as shown in Sec. V, further motivates the validity of this assumption.

IV. EXPERIMENTAL

Three molybdenum mirror samples, including a ScMo (single crystalline molybdenum) sample (20×20 mm) with a (110) crystal orientation, a NcMo (nanocrystalline molybdenum) sample (25 mm round) and a PcMo (polycrystalline molybdenum) sample (20×20 mm) were exposed to deuterium plasma. The term nanocrystalline refers to a type of coating that is produced using magnetron sputtering;^{4,5} the sample used in this work was produced by coating a polished stainless steel surface. The single crystalline samples had been produced by electron beam zone melting in the form of rods, whereas the polycrystalline samples had been produced from sintered molybdenum rolled to size. For more information on the manufacturing of these samples the reader is referred to Ref. 6. The ScMo and PcMo samples were mechanically polished before exposure first by abrasive SiC paper, then by diamond paste and finally by alumina powder with $0.05 \mu\text{m}$ particle size. The resulting surface roughness values, each obtained by averaging five measurements of 1 mm length using a Tencor 500 alpha stepper, are listed in Table I.

The deuterium pressure during exposure was 3 Pa. The mirrors were biased to -200 V and heated passively by the plasma to $80\text{--}85^\circ\text{C}$. From measurements of the mass loss of a molybdenum sample under the same conditions the D^+

TABLE I. Surface roughness and change of diffuse reflectivity of ScMo, NcMo, and PcMo samples before and after exposure to deuterium plasma, measured with an alpha stepper and a spectrophotometer.

	$R_{a,\text{initial}}$ (nm)	$R_{a,\text{final}}$ (nm)	$\Delta R_{\text{diffuse}}$ (%)
ScMo	5.2	5.1	0
NcMo	5.2	6.7	0
PcMo	17.6	91.7	+8... 10

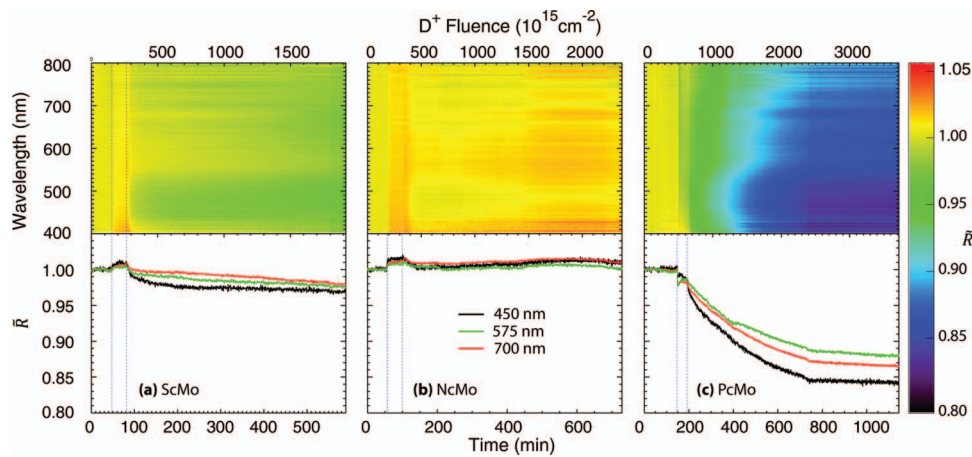


FIG. 4. (Color online) The top panels show the time evolution of the reflectivity spectrum of (a) ScMo, (b) NcMo, and (c) PcMo, between 400 and 800 nm during deuterium exposure, relative to the first time slice. The dashed vertical lines indicate the plasma switch-on, followed by the application of a -200 V bias. The bottom panels show time traces corresponding to three wavelengths, including 450, 575, and 700 nm.

ion flux is estimated at $1.55 \times 10^{15} \text{ cm}^{-2} \text{ s}^{-1}$. The total ion flux, calculated from Langmuir probe measurements, was determined to be $3.25 \times 10^{15} \text{ cm}^{-2} \text{ s}^{-1}$, when the molecular species of deuterium plasma are also included.³ Under these conditions, the erosion rate is known to be typically 0.9–1.0 nm per hour for ScMo and NcMo, though no data are as yet available for PcMo.

The *ex situ* UV–VIS–NIR reflectivity of the mirrors was measured before and after exposure using a Varian Cary 5 spectrophotometer (250–2500 nm) and is shown in Fig. 5(d).

V. RESULTS AND DISCUSSION

The top panels in Fig. 4 show the evolution of the reflectivity spectrum of the ScMo, NcMo, and PcMo samples during deuterium plasma exposure, relative to the first time slice, as a function of wavelength. The time of plasma switch-on and, somewhat later, -200 V bias applications are indicated by dashed vertical lines. The plasma switch-off is not visible in these graphs, showing that the influence of plasma

light is negligible also in the absence of a shutter. The bottom panels show corresponding time traces for three different wavelengths. Figures 5(a)–5(c) show the ratio of the reflectivity spectra before and after exposure, as obtained with the *in situ* reflectometer and from *ex situ* measurements. Figure 5(d) shows the absolute reflectivity spectra before and after exposure, as measured by spectrophotometry. Note that the initial reflectivity of the ScMo and PcMo samples is virtually identical, whereas the NcMo sample has a lower initial reflectivity.

A. Single crystalline molybdenum

As can be seen from Fig. 4(a), the ScMo sample exhibits a small, but gradual decay of the reflectivity between 400 and 800 nm after the bias is applied. In our previous paper³ it was argued that the change in reflectivity during exposure is due to presence of deuterium and defects induced by deuterium in the subsurface. A similar trend was observed with exposures in TEXTOR (Ref. 6) and Tore Supra.⁷ In those cases, it

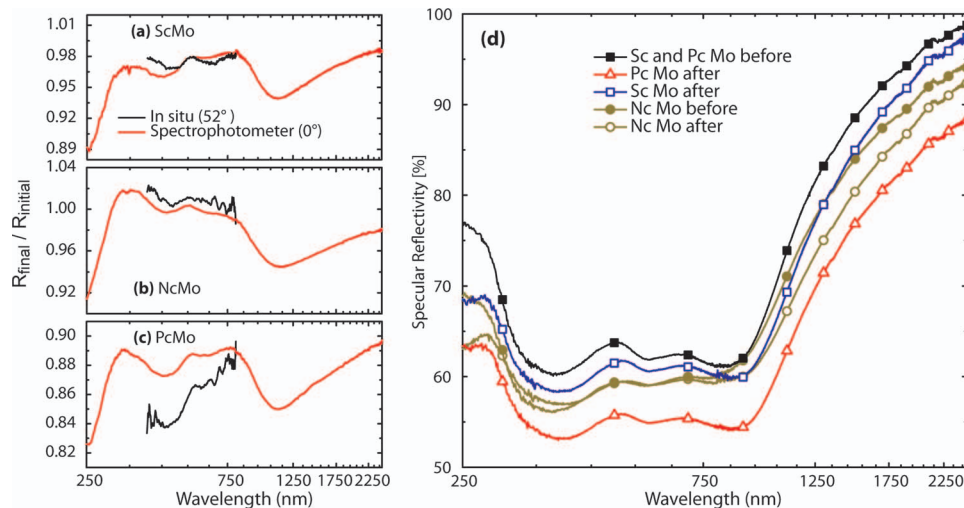


FIG. 5. (Color online) (a)–(c) Final (R_f) divided by initial (R_i) reflectivity spectrum of ScMo, NcMo, and PcMo, obtained from *in situ* reflectometry (black) and spectrophotometry (red). (d) Absolute reflectivity spectra of ScMo and PcMo before exposure (solid black squares), NcMo before exposure (solid brown circles), and likewise after exposure (open blue squares, red triangles, and brown circles, respectively).

was concluded on the basis of *ex situ* x-ray photoelectron spectroscopy (XPS) measurements alone that carbon layer formation was responsible for the decrease in reflectivity, disregarding other possible mechanisms. The results presented here, however, were obtained by using a carbon free plasma, as confirmed by mass spectroscopy measurements and the absence of hydrocarbon emission lines. Also, *in situ* XPS measurements showed no signs of carbon on the surface after exposure. This clearly demonstrates that a reflectivity decrease occurs during a carbon free plasma exposure as well, though this is not to say that carbon layer formation did not contribute in the case of the exposures in TEXTOR and Tore Supra. Surface roughening or an increased diffuse reflectivity after exposure were neither observed in this work nor in any of the ones referred to Refs. 3, 7, and 8 that considered ScMo and Mo coatings produced by magnetron sputtering, see also Table I. In Ref. 3, ScMo was found to display a stable reflectivity during deuterium plasma exposure once a certain fluence had been reached. The exposures in the present work are too short for this effect to be evident.

B. Nanocrystalline molybdenum

The nanocrystalline mirror performed remarkably well. Following an initial increase in reflectivity at plasma switch-on, possibly due to the instantaneous removal of either native oxide or a hydrocarbon layer built up during storage, the reflectivity drops only slightly after the bias is applied and remains virtually constant throughout the exposure (Fig. 4(b)). It has to be kept in mind, however, that this sample had a lower reflectivity to start with (Fig. 5(d)). Previous work³ demonstrated that NcMo coatings produced by magnetron sputtering, such as ScMo, show a stable reflectivity following an initial decrease. This effect is also visible here, though less pronounced due to the lower initial reflectivity.

C. Polycrystalline molybdenum

Previous work⁹ on deuterium exposure of PcMo mirrors reported heavy blistering and/or roughening of the PcMo surface. After the exposure of PcMo in this work, the loss of the specular reflection of the mirror surface was even observable with the bare eye. Optical inspection on the sample revealed that heavy blistering occurred on the surface (Fig. 6) and an enormous increase in surface roughness was measured (Table I). During the exposure the reflectivity had continuously decreased (Fig. 4(c)), unlike in the case of the ScMo and NcMo samples (Figs. 4(a) and 4(b)). This is clearly due to the formation of blisters on the surface. The final reflectivity obtained with the reflectometer is in reasonable agreement with the result from the spectrophotometer. The small difference between two methods may be due to surface processes occurring between removing the samples from the vacuum chamber and measuring their reflectivity using the spectrophotometer, or due to the different angle of incidence used in these measurements, 0° for the spectrophotometer and 52° for the reflectometer, which could have an effect with this degree of roughness.

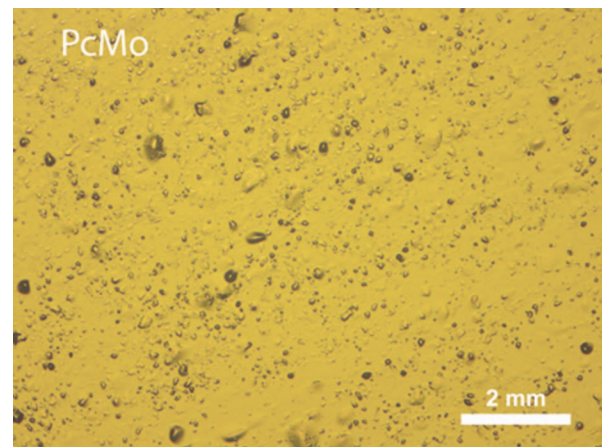


FIG. 6. (Color online) Optical microscope image of the PcMo sample after exposure. Severe blistering is visible on the surface.

VI. CONCLUSION

A new *in situ* spectroscopic reflectometry system has been developed, designed especially to be insensitive to external perturbations induced by thermal stresses. The system has been used to monitor the temporal evolution of the reflectivity of three types of molybdenum mirror samples, including ScMo, NcMo, and PcMo, under deuterium plasma exposure. The results of previous work have been confirmed, showing a stabilisation of the reflectivity of NcMo after an initial deterioration. It has been demonstrated that the decrease of the reflectivity of ScMo and NcMo cannot be attributed to surface roughening or carbon layer formation, and should instead be attributed to the incorporation of deuterium in the surface, as discussed in previous work.³ The dramatic drop in the reflectivity of PcMo due to blistering, as reported by other authors, has been confirmed. Future experiments will see the admixture of impurities in the deuterium plasma to simulate an ITER-like environment and may include tungsten, methane and aluminium or magnesium (as beryllium substitute). In addition, plasma cleaning experiments for mirror surface recovery are scheduled, which will benefit from this new diagnostic.

ACKNOWLEDGMENTS

The authors would like to thank the Swiss Federal Office of Energy and the Federal Office for Education and Science for their financial support. This work was also supported by the Swiss National Foundation (SNF) and the National Center of Competence in Research on Nanoscale Science (NCCR-Nano).

¹A. Litnovsky, P. Wienhold, V. Philipps, G. Sergienko, O. Schmitz, A. Kirschner, A. Kreter, S. Droste, U. Samm, Ph. Mertens, A. H. Donné, D. Rudakov, S. Allen, R. Boivin, A. McLean, P. Stangeby, W. West, C. Wong, M. Lipa, B. Schunke, G. De Temmerman, R. Pitts, A. Costley, V. Voitsenya, K. Vukolov, P. Oelhafen, M. Rubel, and A. Romanyuk, *J. Nucl. Mater.* **363–365**, 1395 (2007).

²A. Litnovsky, V. S. Voitsenya, and A. J. H. Donné, *Nucl. Fusion* **47**, 833 (2007).

³B. Eren, L. Marot, M. Langer, R. Steiner, M. Wisse, D. Mathys, and E. Meyer, *Nucl. Fusion* **51**, 103025 (2011).

- ⁴B. Eren, L. Marot, A. Litnovsky, M. Matveeva, R. Steiner, V. Emberger, M. Wisse, D. Mathys, G. Covarel, and E. Meyer, *Fusion Eng. Des.* **86**, 2593 (2011).
- ⁵L. Marot, G. De Temmerman, V. Thommen, D. Matthys, and P. Oelhafen, *Surf. Coat. Technol.* **202**, 2837 (2008).
- ⁶A. Litnovsky, G. De Temmerman, K. Vukolov, P. Wienhold, V. Philipps, O. Schmitz, U. Samm, G. Sergienko, P. Oelhafen, M. Büttner, I. Orlovskiy, A. Yastrebkov, U. Breuer, and A. Scholl, *Fusion Eng. Des.* **82**, 123 (2007).
- ⁷M. Matveeva, A. Litnovsky, L. Marot, B. Eren, E. Meyer, V. Philipps, A. Pospieszczyk, H. Stoschus, D. Matveev, and U. Samm, *Proceedings of the 37th EPS Conference on Plasma Physics and Controlled Fusion*, Dublin, 2011, P2.105.
- ⁸M. Lipa, B. Schunke, Ch. Gil, J. Bucalossi, V. S. Voitsenya, V. Konovalov, K. Vukolov, M. Balden, G. De Temmerman, P. Oelhafen, A. Litnovsky, and P. Wienhold, *Fusion Eng. Des.* **81**, 221 (2006).
- ⁹T. Sugie, S. Kasaia, M. Taniguchia, M. Nagatsub, and T. Nishitania, *J. Nucl. Mater.* **329–333**, 1481 (2004).